Supplementary Information

Terpyridine–Thiophene–Triphenylamine Conjugated Ligand Design Enabling Green-Colored, Multistate Electrochromic Fe(II) Metallopolymers

Gihyeok Bak, Yu Jin Jung*, and Hanah Na*

Center for Advanced Specialty Chemicals, Korea Research Institute of Chemical Technology, Ulsan, 44412, Republic of Korea

*Corresponding author
*Email: yjjung@krict.re.kr
*Email: hanah@krict.re.kr

Table of contents

1. General specifications

Materials and Reagents

2-Acetylpyridine (98%), bis(pinacolato)diborane (≥ 98%), potassium acetate (CH_3COOK, ≥ 99%), , tetrabutylammonium hexa-fluorophosphate ($TBAPF_6$, 98%), and iodine (I_2, ≥ 99%) were purchased from Thermo Scientific. 3-Bromothiophene-2-carboxaldehyde (≥ 98%), pyridine (≥ 99%), and basic aluminium oxide (~ 60 mesh) were obtained from Alfa Aesar. 4-Bromo-*N,N*-triphenylaniline (≥ 97%) was supplied by TCI Co. Ltd. (Japan). $Pd(dppf)Cl_2$, $Pd(PPh_3)_4$ (99%), silica gel (70 ~ 230 mesh, 63 ~ 200 μm, pore size 60 Å), activated charcoal (untreated, granular, 8–20 mesh), ammonium acetate (NH_4OAc), and iron(II) tetrafluoroborate hexahydrate ($FeBF_4 \cdot 6H_2O$) were purchased from Merck/Sigma-Aldrich. Potassium hydroxide (KOH, 95%), potassium carbonate (K_2CO_3, 99.5%), magnesium sulfate ($MgSO_4$, 99.5%), methanol (MeOH, 99.9%), 1,4-dioxane (99.5%), n-hexane (95%), acetone (99.5%), and ethyl acetate (EA, 99.5%) were obtained from SAMCHUN Chemicals (Republic of Korea). Tetrahydrofuran (THF, ≥ 99.9%), acetonitrile (MeCN, ≥ 99.9%), and isopropyl alcohol (IPA, ≥ 99.9%) were purchased from Burdick & Jackson. $TBAPF_6$ used for electrochemical experiments was recrystallized three times from hot EA and dried overnight under vacuum at 85 °C prior to use. Indium tin oxide (ITO)-coated glass substrates (8 × 40 mm, 0.7 mm thickness, 10 Ω/sq, OMNI-SCIENCE) were used for electropolymerization and spectro-electrochemical analyses. Prior to use, substrates were ultrasonically cleaned for 15 min each in deionized water, acetone, and IPA, followed by drying in an oven at 60 °C for at least 6 h.

Characterization Methods

Proton nuclear magnetic resonance (^1H NMR) spectra were recorded on Bruker Avance 300 or 600 MHz spectrometers using deuterated chloroform ($CDCl_3$) or acetonitrile (CD_3CN). Fluorine NMR (^{19}F NMR) spectra were obtained using a Bruker Avance 565 MHz

spectrometer with CD_3CN as a solvent. Elemental analysis (CHN) was performed using a Flash 2000 automatic elemental analyzer (Thermo Fisher Scientific) at the Technical Support Center for the Chemical Industry, KRICT. UV-vis-near-infrared (UV-vis-NIR) absorption and transmittance spectra were collected using a SEC2020 spectrophotometer (ALS Co., Ltd.). Electrochemical measurements, including cyclic voltammetry (CV) and electropolymerization, were performed using a CH Instruments 604E potentiostat in a standard three-electrode configuration. A 3 mm diameter glassy carbon electrode (or ITO glass), Pt wire, and silver wire were used as working electrode, counter electrode, and pseudoreference electrode, respectively. Measurement were carried out in electrolyte solution containing 0.1 M $TBAPF_6$ in MeCN. Ferrocene was used as an internal standard, and potentials were referenced to the ferrocene/ferrocenium couple. Spectro-electrochemical (SEC) and chronoamperometry (CA) measurements were conducted using a coupled SEC2020 spectrophotometer and CH Instruments 604E potentiostat, employing a 1 cm quartz optical cuvette containing 0.1 M $TBAPF_6$ in MeCN. Top-view SEM images and SEM-EDS analysis of metallopolymer-coated ITO substrates were acquired using the TESCAN MIRA 3 LMH scanning electron microscope with an in-beam detector at an accelerating voltage of 15 kV after Pt coating of the samples. X-ray photoelectron spectroscopy (XPS) measurements were carried out using a Thermo Fisher Scientific instrument equipped with a monochromated Al Kα source, a double-focusing hemispherical analyzer, and a 250 mm Rowland circle monochromator.

Chronoamperometry

Chronoamperometry (CA) was performed in 0.1 M $TBAPF_6$/MeCN using square-wave potential steps. Fe metallopolymer films (Poly-Fe) were electropolymerized onto ITO-glass substrates with an effective coated area of 0.72 cm^2, which was used to calculate current density values. The potentials were alternated between –0.3 and 1.0 or 1.2 V (vs $Fc^{+/0}$) with a pulse

width of 10 s. A total of 10 switching cycles were conducted to determine the coloration (t_c) and bleaching (t_b) response times, as well as the optical contrast (ΔT). Electrochromic switching durability was further examined by applying the same potential steps for 300 consecutive cycles.

2. Synthesis

Reactions were performed in ambient conditions unless otherwise stated. All starting materials and reagents, unless otherwise specified, were obtained from commercial sources and used without further purification. 4′-(5-Bromo-2-thienyl)-2,2′:6′,2″-terpyridine (TpyThBr) and N,N-Diphenyl-4-(4,4,5,5-tetramethyl-1,3,2-dioxaborolan-2-yl)benzenamine (TPA-Bpin) was prepared according to previously published procedure [1, 2]. Previously reported compounds $[Fe^{II}(Tpy)_2]^{2+}$ and $[Fe^{II}(TpyTh)_2]^{2+}$ were synthesized according to literature procedures[3].

Synthesis of TpyThTPA ligand (**2**): The target organic ligand was synthesized via a Suzuki cross-coupling reaction. TpyThBr (**1**) (210 mg, 0.533 mmol), TPA-Bpin (217 mg, 0.584 mmol), $Pd(PPh_3)_4$ (61.0 mg, 0.053 mmol), and K_2CO_3 (0.70 g, 5.06 mmol) were added to a flask, and a nitrogen atmosphere was established using a Schlenk line. A mixture of THF and deionized water (9:1 v/v, 18.9 mL) was added, degassed with nitrogen, and then stirred and refluxed at 80 °C for 14 h. After cooling to room temperature, the reaction mixture was diluted with deionized water and extracted with CH_2Cl_2. The organic phase was dried over anhydrous $MgSO_4$, filtered, and concentrated. The crude product was purified by column chromatography using CH_2Cl_2/n-hexane (1:4 to 1:0 v/v) as the eluent and basic aluminium oxide as the stationary phase to afford the ligand TpyThTPA as a deep yellow solid (0.380 g, yield: 64.4%). ^{1}H NMR (300 MHz, $CDCl_3$) δ [ppm] = 8.78 - 8.73 (m, 4H), 8.70 (d, J = 8.0 Hz, 2H), 7.95 - 7.89 (td, J = 7.7, 1.8 Hz, 2H), 7.82 - 7.80 (d, J = 3.9 Hz, 1H), 7.56 - 7.52 (m, 2H), 7.42 - 7.37

(ddd, J = 7.5, 4.9, 1.2 Hz, 2H), 7.32 - 7.29 (m, 5H), 7.16 - 7.03 (m, 8H). ^{13}C NMR (125 MHz, $CDCl_3$) δ [ppm] = 156.21, 156.13, 149.26, 147.89, 147.50, 146.13, 143.49, 139.94, 136.99, 129.50, 127.91, 127.01, 126.74, 124.83, 124.02, 123.51, 123.42, 123.38, 121.46, 116.73. ^{1}H and ^{13}C NMR spectra are consistent with previously reported data [4].

Synthesis of $[Fe^{II}(TpyThTPA)_2](BF_4)_2$ (**3**): The target monomeric Fe(II) complex, compound **3**, was obtained via metal coordination synthesis. In a vial, compound **2** (2.0 equiv) and $Fe(BF_4)_2{\cdot}6H_2O$ (1.0 equiv) were dissolved in MeCN (5.0 mL). The reaction mixture was stirred at room temperature for at least 4 h. After completion of the reaction, diethyl ether (15.0 mL) was slowly added to the reaction mixture to induce precipitation. The dark-green precipitate was collected by vacuum filtration and dried under vacuum to afford the Fe(II) coordination complex (110.0 mg, yield: 91.9%). ^{1}H NMR (600 MHz, CD_3CN) δ [ppm] = 9.07 (s, 4H, tpy H3′, H5′), 8.62–8.60 (dt, J = 8.1, 1.1 Hz, 4H, tpy H3, H3″), 8.28–8.27 (d, J = 3.9 Hz, 2H, Th H), 7.92–7.89 (td, J = 7.8, 1.5 Hz, 4H, tpy H4, H4″), 7.75 - 7.73 (m, 4H, tpy H6, H6″), 7.65 (d, J = 3.9 Hz, 2H, Th H), 7.39–7.37 (m, 8H, (4H tpy H5′, H5″ + 4H from Th-*Ph*-N), 7.22–7.21 (ddd, J = 5.7, 1.5, 0.7 Hz, 4H, Th-*Ph*-N), 7.18–7.15 (m, 12H, N-*Ph*), 7.12–7.07 (m, 8H N-*Ph*). ^{13}C NMR (151 MHz, $CDCl_3$) δ [ppm] = 161.06 (tpy *C*=N), 158.82 (tpy *C*=N), 154.03 (tpy *C*=N), 149.67 (tpy *C*–Th), 149.43 (Th *C*–tpy), 148.09 (tpy *C*–H), 144.20 (tpy *C*–H), 139.63 (tpy *C*–H), 138.47 (tpy *C*–H), 131.13 (Th *C*–TPA), 130.58 (TPA Ph *C*–H), 128.25 (Th *C*–H), 127.82 (Th *C*–H), 127.42 (TPA *C*–N), 126.04 (TPA Ph *C*–H), 125.51 (TPA *C*–N), 124.95 (TPA Ph *C*–H), 124.77 (TPA Ph *C*–H), 123.34 (TPA Ph *C*–H), 119.84 (TPA Ph *C*–H). ^{19}F NMR (565 MHz, CD_3CN) δ [ppm] = –151.655 (d, J = 30.1 Hz). Elemental analysis: Anal. Calcd for $C_{74}H_{52}B_2F_8FeN_8S_2{\cdot}2CH_3CN$; C, 65.56; H, 4.09; N, 9.80; S, 4.48. Found: C, 65.49; H, 4.25; N, 9.64; S, 4.32. HRMS-ESI (*m/z*): $[M\text{-}(BF_4)_2]^{2+}$ calcd for 586.1553; found 586.1554, $[M\text{-}(BF_4)]^{+}$ calcd for 1259.3135; found 1259.3140.

Electropolymerization for preparing Poly-Fe film (4) : Metallopolymer films were prepared via electrochemical polymerization using ITO-coated glass substrates as working electrodes. Cyclic voltammetry was conducted in a 0.1 M $TBAPF_6$/anhydrous CH_2Cl_2 electrolyte solution containing 0.5 mM of the monomer complex $[Fe^{II}(TpyThTPA)_2](BF_4)_2$ (**3**). The potential window was –0.36 to 1.24 V vs $Fc^{+/0}$ and was scanned at 100 mV s^{-1} for the designated number of cycles. The resulting films were rinsed three times with anhydrous CH_2Cl_2 and dried at 50 °C for 1 h, followed by overnight drying under vacuum at room temperature.

3. NMR spectra

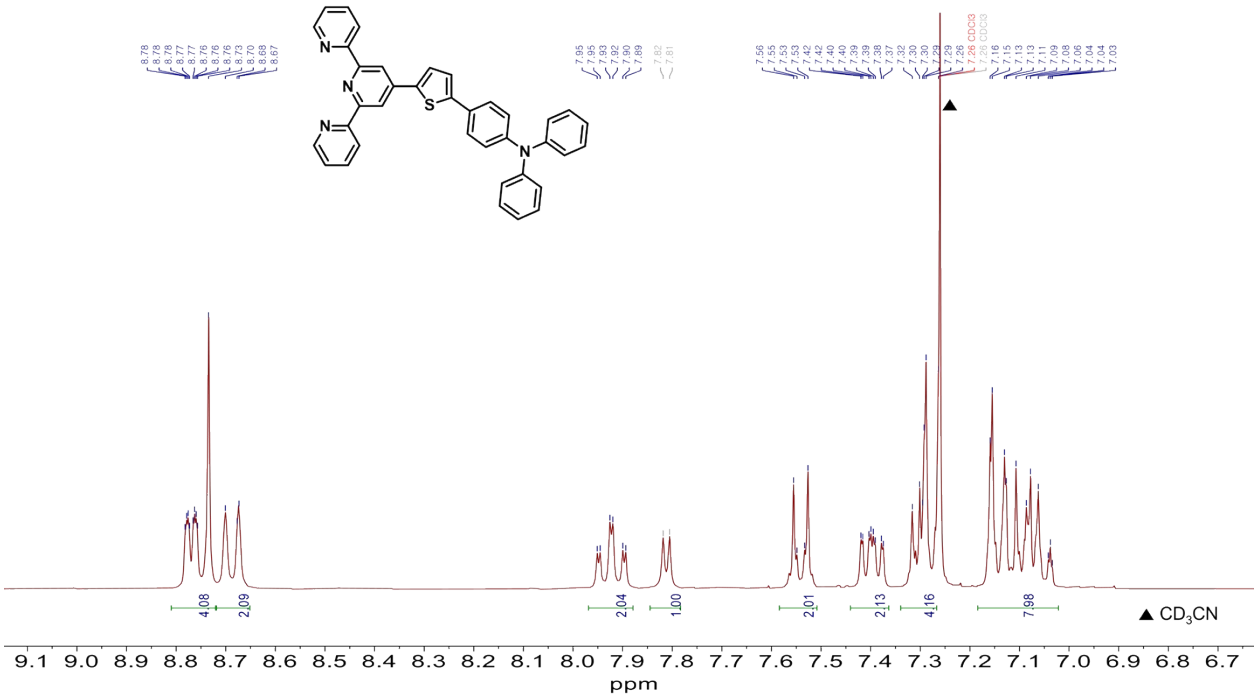

Figure S1. ^{1}H NMR spectrum of TpyThTPA recorded in $CDCl_3$ at 300 MHz

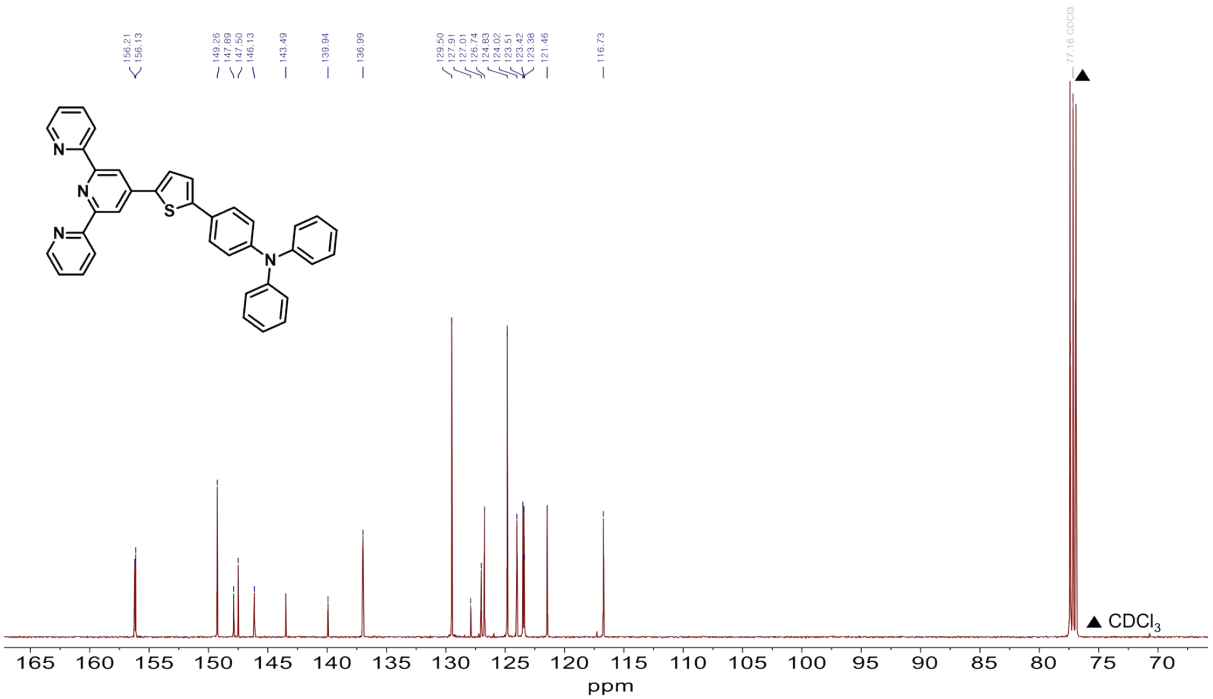

Figure S2. ^{13}C NMR spectrum of TpyThTPA recorded in $CDCl_3$ at 125 MHz

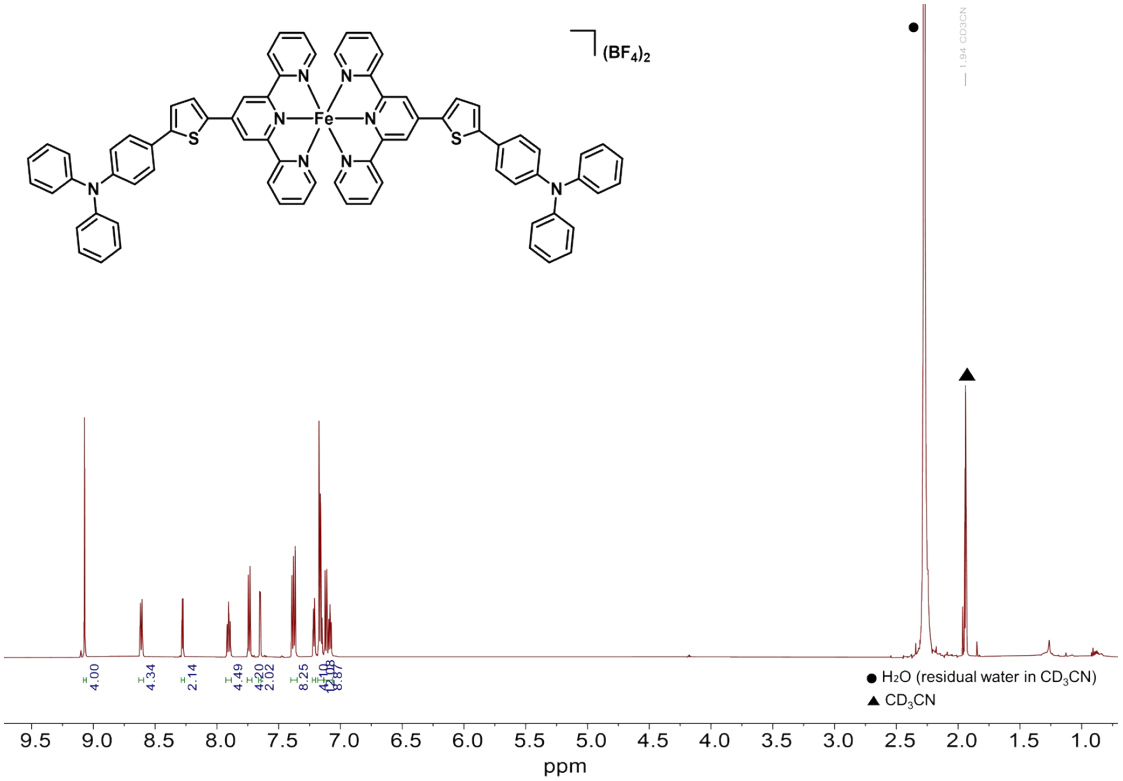

Figure S3. ^{1}H NMR spectrum of $[Fe^{II}(TpyThTPA)_2](BF_4)_2$ (**3**) recorded in CD_3CN at 600 MHz

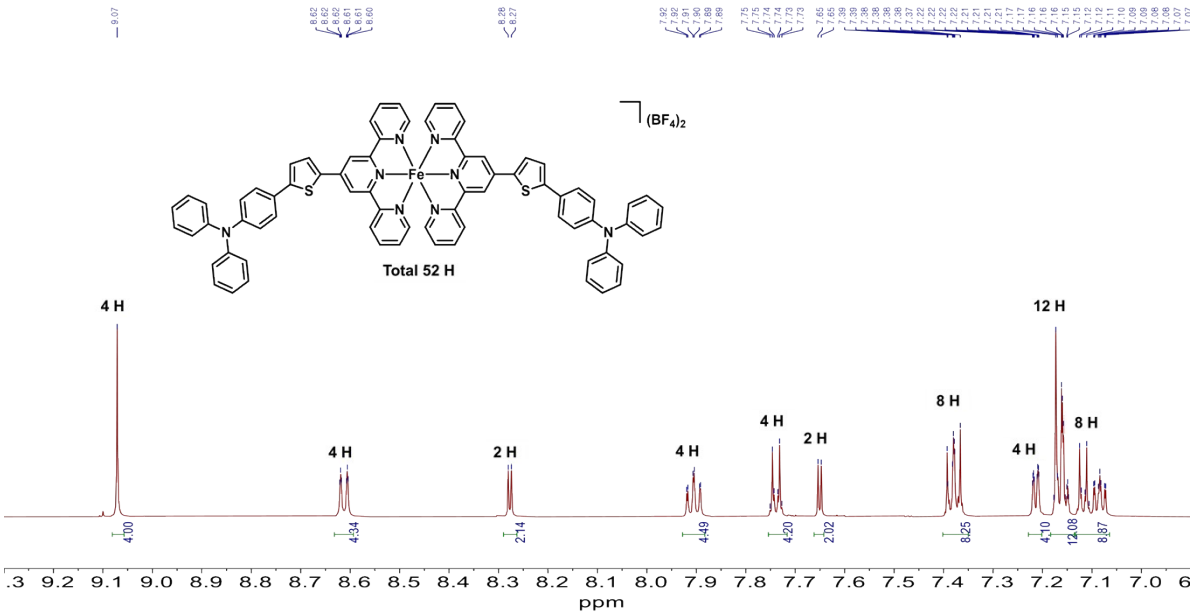

Figure S4. Expanded view of ^{1}H NMR spectrum of $[Fe^{II}(TpyThTPA)_2](BF_4)_2$ (**3**) recorded in CD_3CN at 600 MHz. δ [ppm] = 9.07 (s, 4H, tpy H3′, H5′), 8.62–8.60 (dt, J = 8.1, 1.1 Hz, 4H, tpy H3, H3″), 8.28–8.27 (d, J = 3.9 Hz, 2H, Th H), 7.92–7.89 (td, J = 7.8, 1.5 Hz, 4H, tpy H4, H4″), 7.75 - 7.73 (m, 4H, tpy H6, H6″), 7.65 (d, J = 3.9 Hz, 2H, Th H), 7.39–7.37 (m, 8H, (4H tpy H5′, H5″ + 4H from Th-*Ph*-N), 7.22–7.21 (ddd, J = 5.7, 1.5, 0.7 Hz, 4H, Th-*Ph*-N), 7.18–7.15 (m, 12H, N-*Ph*), 7.12–7.07 (m, 8H N-*Ph*).

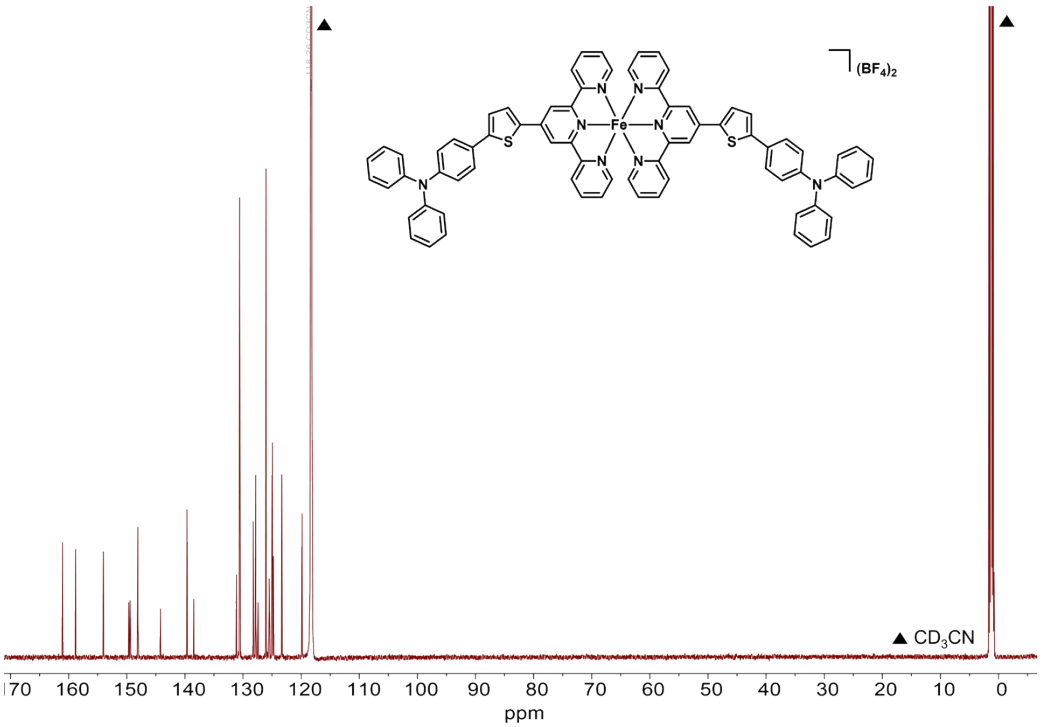

Figure S5. ^{13}C NMR spectrum of $[Fe^{II}(TpyThTPA)_2](BF_4)_2$ (**3**) recorded in CD_3CN at 151 MHz

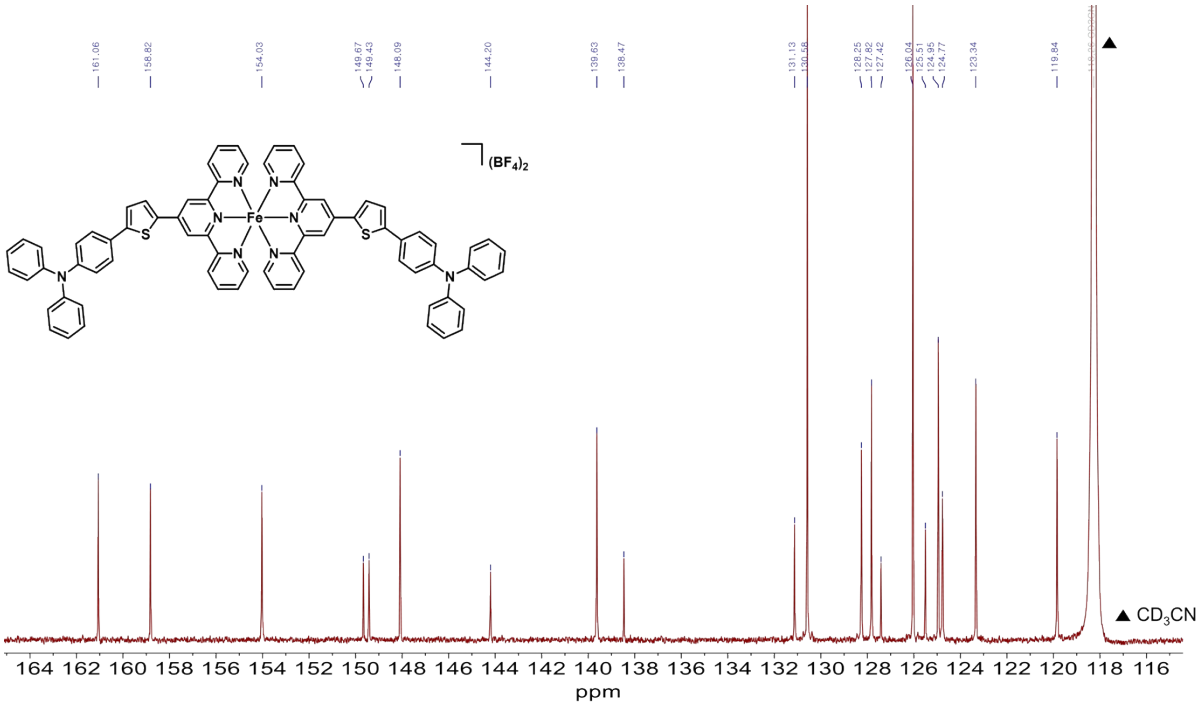

Figure S6. Expanded view of ^{13}C NMR spectrum of $[Fe^{II}(TpyThTPA)_2](BF_4)_2$ (**3**) recorded in CD_3CN at 151 MHz. δ [ppm] = 161.06 (tpy *C*=N), 158.82 (tpy *C*=N), 154.03 (tpy *C*=N), 149.67 (tpy *C*–Th), 149.43 (Th *C*–tpy), 148.09 (tpy *C*–H), 144.20 (tpy *C*–H), 139.63 (tpy *C*–H), 138.47 (tpy *C*–H), 131.13 (Th *C*–TPA), 130.58 (TPA Ph *C*–H), 128.25 (Th *C*–H), 127.82 (Th *C*–H), 127.42 (TPA *C*–N), 126.04 (TPA Ph *C*–H), 125.51 (TPA *C*–N), 124.95 (TPA Ph *C*–H), 124.77 (TPA Ph *C*–H), 123.34 (TPA Ph *C*–H), 119.84 (TPA Ph *C*–H).

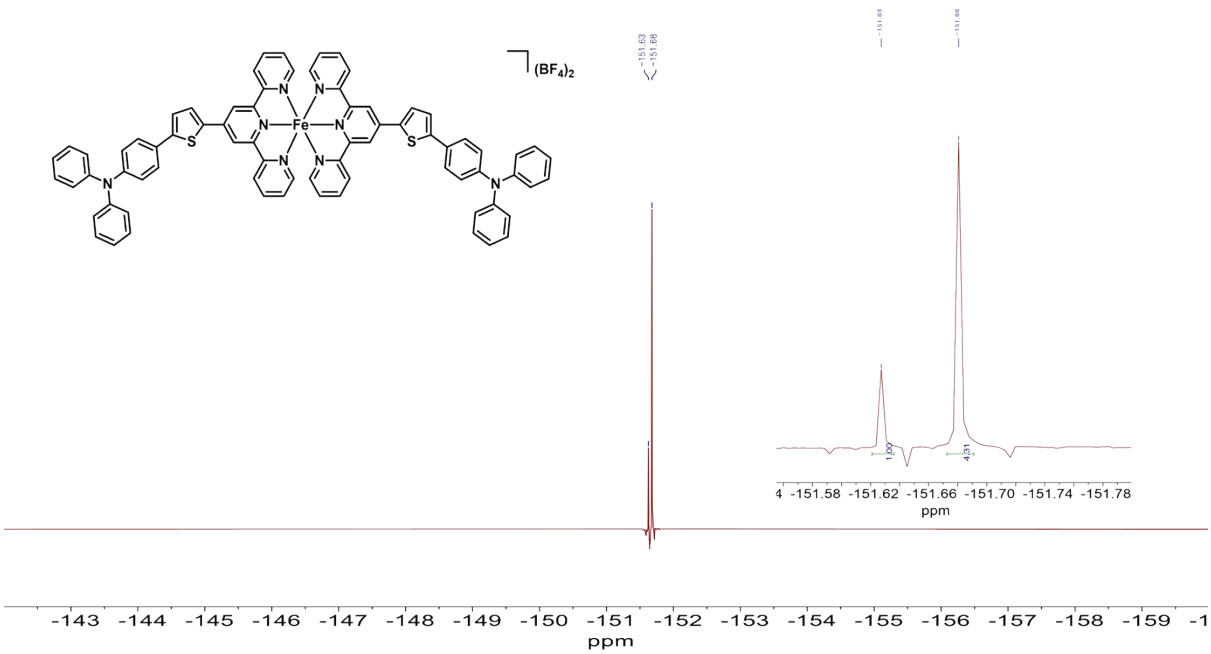

Figure S7. ^{19}F NMR spectrum of $[Fe^{II}(TpyThTPA)_2](BF_4)_2$ (**3**) recorded in CD_3CN at 565 MHz

4. Absorption spectra of Fe monomer complexes

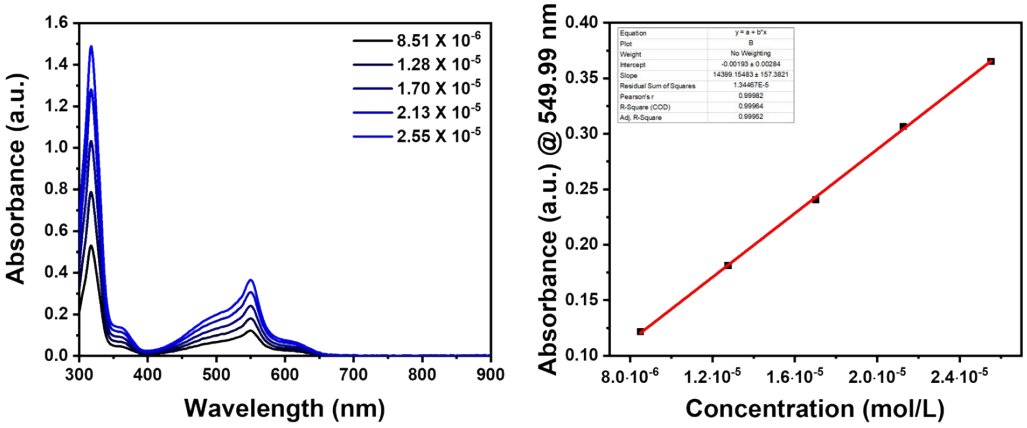

Figure S8. Absorption spectrum of $[Fe^{II}(Tpy)_2](BF_4)_2$ measured in CH_3CN (left), and concentration-dependent absorbance with the corresponding molar extinction coefficient (ε) (right).

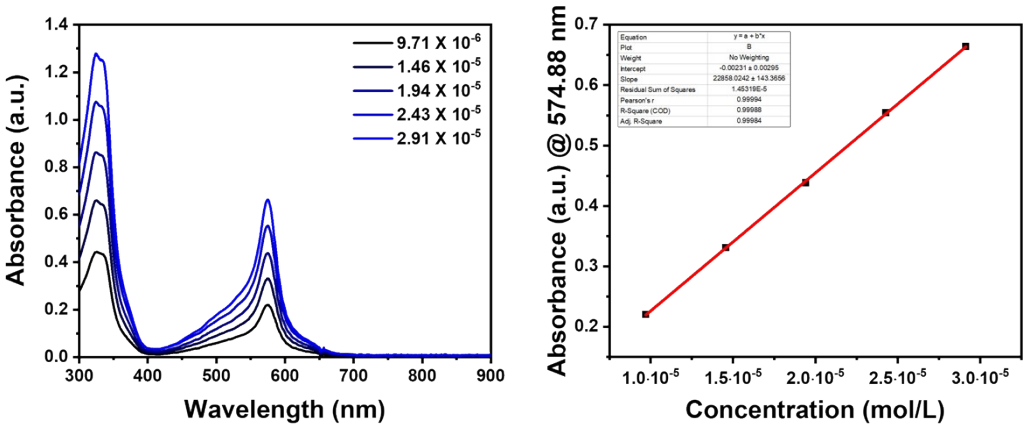

Figure S9. Absorption spectrum of $[Fe^{II}(TpyTh)_2](BF_4)_2$ measured in CH_3CN (left), and concentration-dependent absorbance with the corresponding molar extinction coefficient (ε) (right).

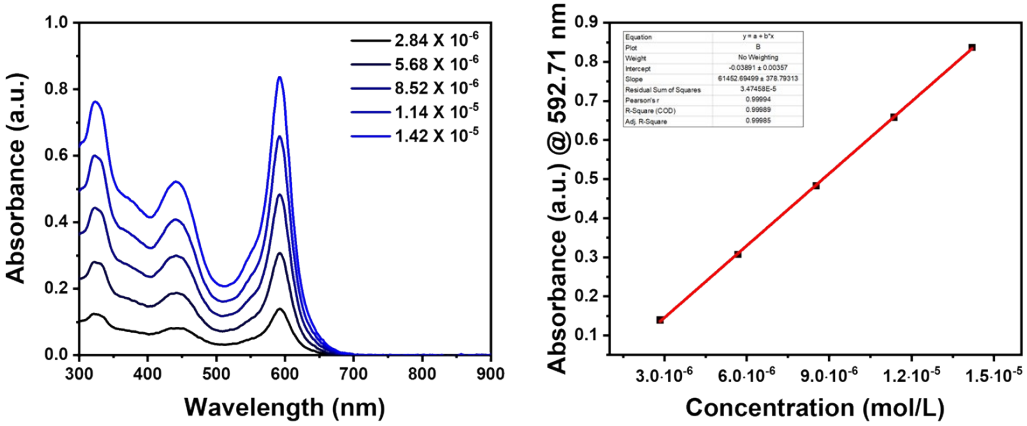

Figure S10. Absorption spectrum of $[Fe^{II}(TpyThTPA)_2](BF_4)_2$ (**3**) measured in CH_3CN (left), and concentration-dependent absorbance with the corresponding molar extinction coefficient (ε) (right).

5. Proposed electropolymerization pathway

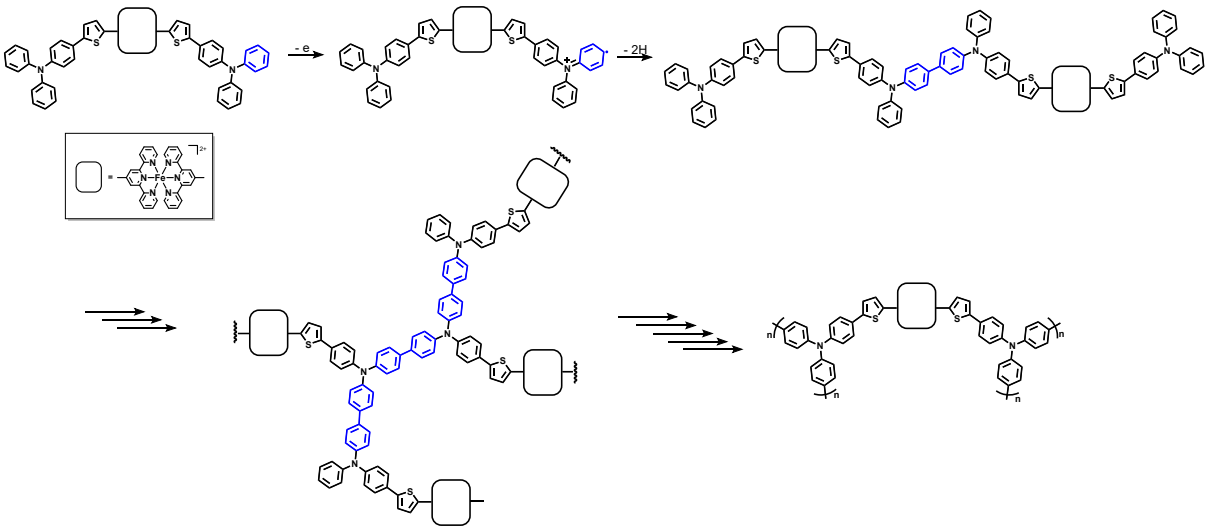

Figure S11. Proposed electropolymerization pathway of the Fe monomer (**3**) containing two triphenylamine groups. The notation (–)n represents an idealized repeating unit ($[Fe^{II}(TpyThTPA)_2]^{2+}$) within the electropolymerized network rather than a strictly linear polymer or a fully defined cross-linked structure.

6. SEM analysis

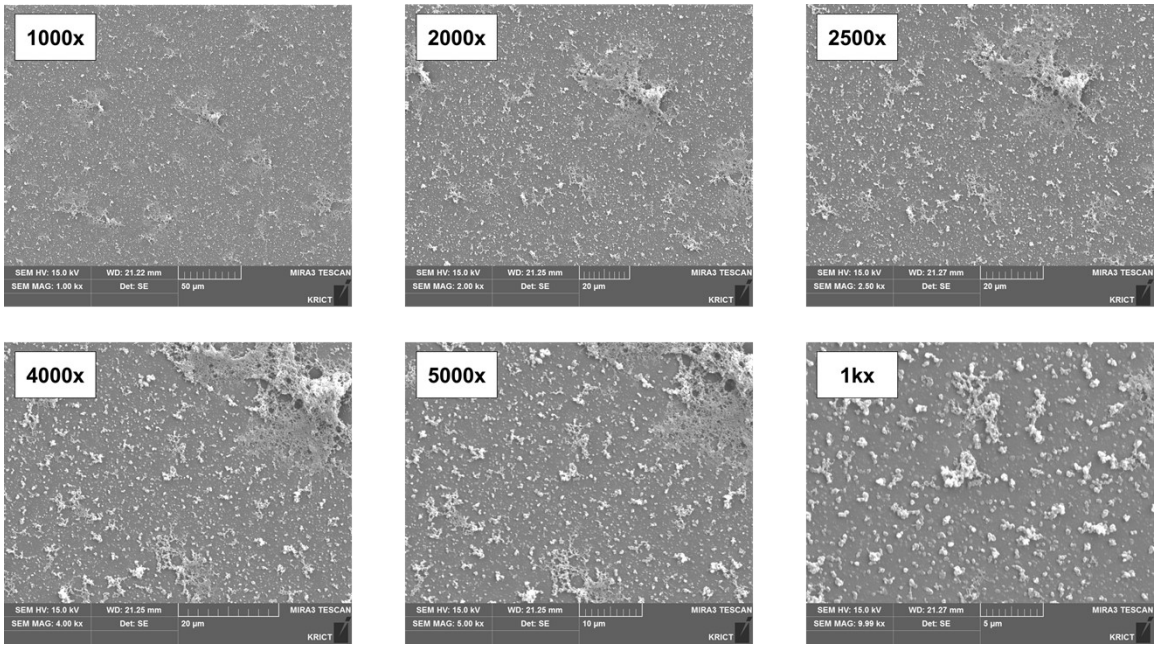

Figure S12. SEM images showing the surface morphology of the metallopolymer Poly-Fe film (**4**) fabricated with 60 cycles.

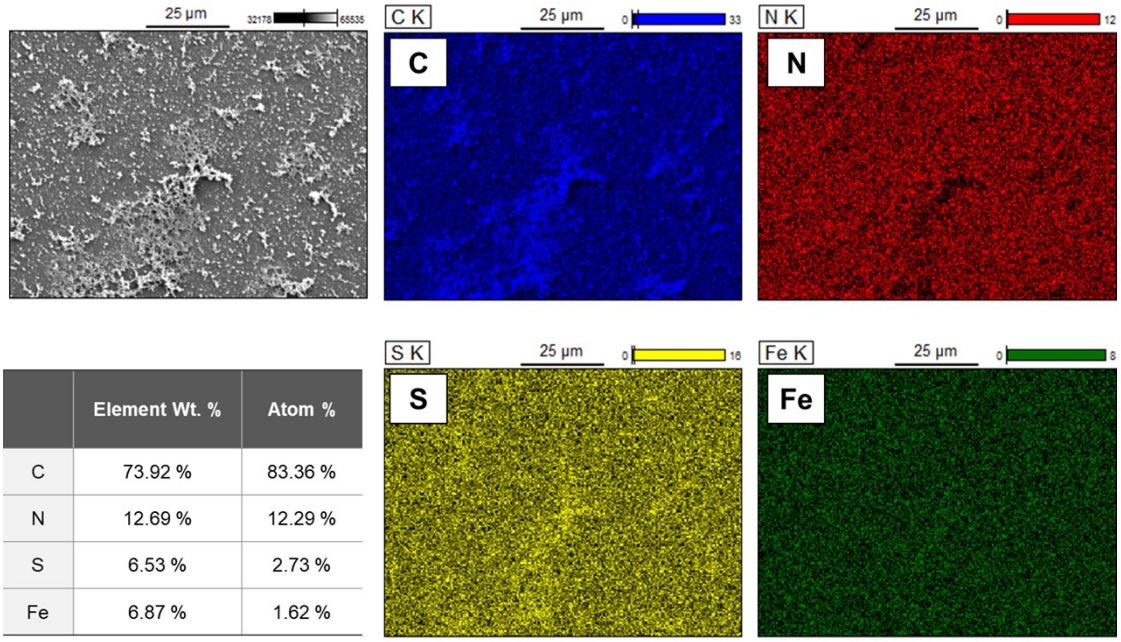

	Element Wt. %	Atom %
C	73.92 %	83.36 %
N	12.69 %	12.29 %
S	6.53 %	2.73 %
Fe	6.87 %	1.62 %

Figure S13. SEM-EDS elemental mapping and quantitative analysis of the metallopolymer Poly-Fe film (**4**).

7. XPS analysis

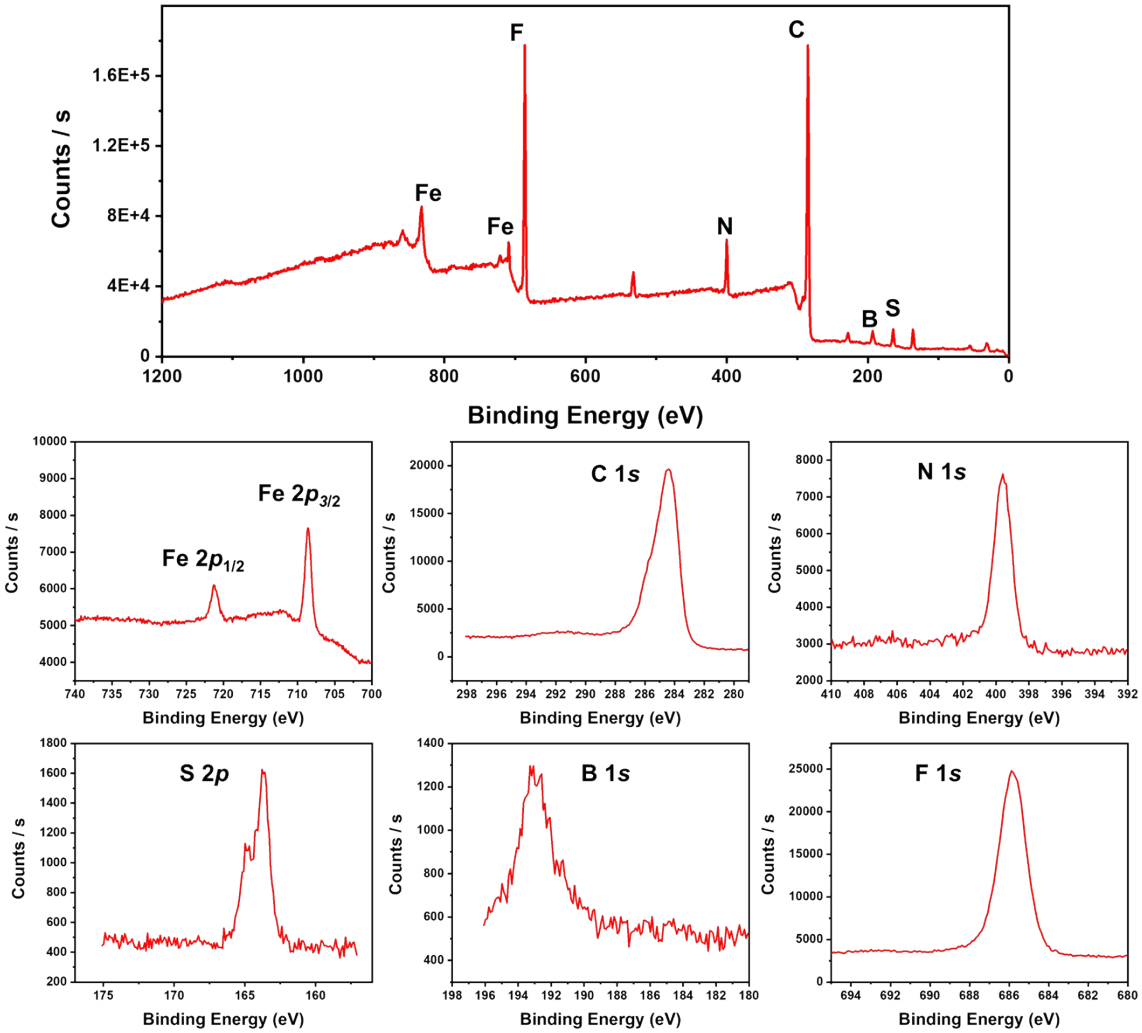

Figure S14. XPS survey and spectra (C 1*s*, N 1*s*, S 2*p*, B 1*s*, F 1*s*, and Fe 2*p*) of the metallopolymer Poly-Fe film (**4**). *Note*: Peaks at 136.1 eV (P 2*p*, from the electrolyte PF_6^-), 228.08 eV (S 2s), and 532.08 eV (O 1s).

8. Color sequence and cycling stability of the Poly–Fe film

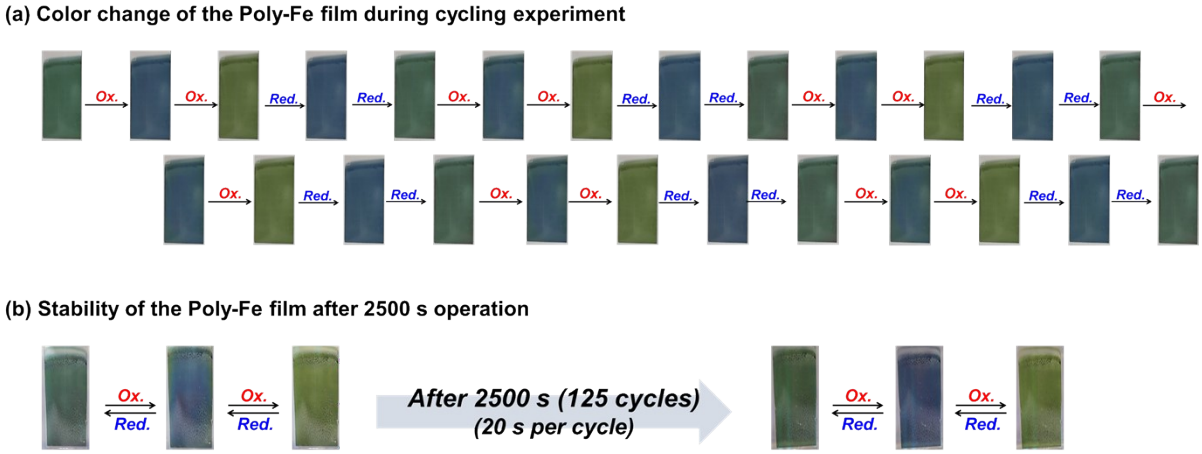

Figure S15. (a) Photographs of the Poly–Fe film (**4**) during electrochromic switching under repeated potential cycling. (b) Photographs of the Poly–Fe film (**4**) at the initial state and after 2500 s of operation (125 cycles, 20 s per cycle).

8. References

1. Kervella, Y., et al., *S-Shaped Conformation of the Quaterthiophene Molecular Backbone in Two-Dimensional Bisterpyridine-Derivative Self-Assembled Nanoarchitecture.* Langmuir, 2015. **31**(49): p. 13420-13425.
2. Xiao, Y., et al., *3D-Printable organic room-temperature phosphorescent elastomers based on N-ethylcarbazole derivatives.* Materials Chemistry Frontiers, 2025. **9**(21): p. 3228-3236.
3. Liang, Y., et al., *A Thiophene-Containing Conductive Metallopolymer Using an Fe(II) Bis(terpyridine) Core for Electrochromic Materials.* ACS Applied Materials & Interfaces, 2016. **8**(50): p. 34568-34580.
4. Robson, K.C.D., et al., *Triphenylamine-Modified Ruthenium(II) Terpyridine Complexes: Enhancement of Light Absorption by Conjugated Bridging Motifs.* Inorganic Chemistry, 2010. **49**(12): p. 5335-5337.